The homeobox transcription factor HB9 induces senescence and blocks differentiation in hematopoietic stem and progenitor cells

Deborah Ingenhag,[1] Sven Reister,[1] Franziska Auer,[1] Sanil Bhatia,[1] Sarah Wildenhain,[1] Daniel Picard,[1,2] Marc Remke,[1,2] Jessica I. Hoell,[1] Andreas Kloetgen,[1,3] Dennis Sohn,[4] Reiner U. Jänicke,[4] Gesine Koegler,[5] Arndt Borkhardt[1] and Julia Hauer[1]

[1]Department of Pediatric Oncology, Hematology and Clinical Immunology, Medical Faculty of Heinrich-Heine-University, Düsseldorf; [2]Department of Pediatric Neuro-Oncogenomics, German Cancer Consortium (DKTK) and German Cancer Research Center (DKFZ), Heidelberg; [3]Computational Biology of Infection Research, Helmholtz Center for Infection Research, Braunschweig; [4]Laboratory of Molecular Radiooncology, Clinic and Policlinic for Radiation Therapy and Radiooncology, Medical Faculty of Heinrich-Heine-University, Düsseldorf and [5]Institute for Transplantation Diagnostics and Cell Therapeutics, Medical Faculty of Heinrich-Heine-University, Düsseldorf, Germany

Supplementary Methods

Virus production

The cDNA sequence of HB9 (NM_005515.3) was obtained from GeneArt (Regensburg, Germany) and cloned into lentiviral vector pCDH-EF1-T2A-copGFP (System Biosciences, Palo Alto, CA, USA). Lentiviral vectors and third generation packaging plasmids [1] were transfected into 293T cells (ACC-635, DSMZ, Braunschweig, Germany) using Polyethylenimin (10µg/ml, Sigma-Aldrich, Taufkirchen, Germany). Transfection was performed overnight. Viral supernatant was harvested 48h and 72h after transfection and concentrated. Virus titer was determined by flow cytometric analysis of HT1080 (ACC-315, DSMZ) or NIH3T3 (ACC-59, DSMZ), infected with serial dilutions.

***In Vitro* growth assays**

HT1080 and NIH3T3 were cultivated in DMEM-GlutaMax (Thermo Fisher Scientific, Darmstadt, Germany) supplemented with 10% FBS and 1% penicillin-streptomycin. After thawing, cells were analyzed for absence of mycoplasmas using VenorGeM Classic Mycoplasma Detection Kit (Minerva Biolabs, Berlin, Germany), according to the manufacturer's instructions, and used for experiments within six weeks. Cells were transduced with a MOI of 7 and hexadimethrine bromide (5µg/ml, Sigma-Aldrich). One day after lentiviral infection, 1×10^4 (NIH3T3) or 2×10^4 (HT1080) cells were plated into flat bottom 48-well plates. Triplicates were counted daily over a period of four days using cell counter (Vi-CELL XR, Beckman-Coulter, Krefeld, Germany).

Immunofluorescence

Cells were plated into 8-well chamber slides (BD Biosciences, Heidelberg, Germany) and sub-confluent cultures were fixed (2% Histofix, Carl Roth, Karlsruhe, Germany) for 10 minutes at room temperature (RT). Cells were permeabilized with 0.1% Triton-X 100 in PBS for 10 minutes, subsequently blocked with 5% FBS for 30 minutes, and incubated with HB9 antibody (H-20, Santa Cruz, Heidelberg, Germany; 1:50 in 2% FBS) for 2h at RT. After a three times-wash with PBS, cells were counterstained with Phalloidin-AF660 (Life Technologies, Darmstadt, Germany) and secondary antibody donkey-anti-goat AF594 (cat. #A27016, Life Technologies) for 1h at RT. After incubation, cells were washed with PBS and mounted with "ProLong Gold Antifade Mountant with DAPI" (Life Technologies). Image acquisition was done using AxioObserver Z1 microscope (Zeiss, Jena, Germany).

siRNA-transfection

HT1080 cells were transfected with 35nM p53 siRNA (ON-TARGETplus TP53 siRNA, Dharmacon, Lafayette, CO, USA) or non-targeting siRNA (ON-TARGETplus non-targeting control, Dharmacon) using Dharmafect 4 transfection reagent according to the manufacturer's instructions, 8h before lentiviral transduction.

Animals

Animals were housed in the animal facility of Heinrich-Heine-University (Duesseldorf, Germany). B6.SJL-Ptprc Pepc/BoyJ mice were bred in-house. C57BL/6 mice were obtained from Janvier Labs (Le Genest-Saint-Isle, France). This study was approved by the "Nordrhein Westfalen Landesamt für Natur, Umwelt und Verbraucherschutz" (Recklinghausen, Germany) and carried out in accordance with the German law for animal protection.

Cell preparation and flow cytometric analysis

Murine blood samples were collected by puncture of the retro-orbital plexus using heparinized capillaries under inhalation anesthesia with isoflurane. White blood cells (WBC) were counted using Türk's solution (Merck Millipore, Darmstadt, Germany) in a Neubauer counting chamber. For each staining, blood volume equivalent to $6*10^4$ WBC was incubated with fluorochrome-labelled antibodies for 20 minutes at 4°C in the dark, followed by ammoniumchloride-based erythrocyte lysis and two-times wash (PBS+0.5% FBS). For bone marrow cell preparation, femur and tibia were flushed with medium and cell suspension was filtered using a 70 µm mesh, followed by erythrocyte lysis. For preparation of thymocytes and splenocytes, tissues were mechanically homogenized using a 100 µm mesh and a plunger of a 2 ml syringe. Splenocyte suspension was further subjected to erythrocyte lysis. For each staining $5*10^5$ cells were pelleted, resuspended in PBS/0.5% FBS and incubated with antibodies for 20 minutes at 4°C in the dark. For analysis of stem and progenitor cells, $4*10^6$ cells were stained accordingly, followed by counterstaining with streptavidin-PerCP-Cy5.5 for 15 minutes. Monitoring of hematopoietic reconstitution in peripheral blood was conducted using a FACS Calibur cytometer (BD Biosciences) and final analysis of all hematopoietic tissues was performed on a CyAn ADP Analyzer (Beckman Coulter, Krefeld, Germany), allowing parallel analysis of up to 8 markers. Antibody-panels used for flow cytometric analyses are given in tables at the end of the supplementary method section.

Western Blot

Cells were lyzed using RIPA (150mM Sodium chloride; 1.0% Igepal; 0.5% Sodium deoxycholate; 0.1% SDS; 50mM Tris, pH 8.0) buffer, containing 1mM DTT, protease- as well as phosphatase-inhibitors (Roche, Penzberg, Germany). Protein

concentrations were measured using Bradford protein reagent (BioRad, Munich, Germany). 30µg of protein were run on a 12% polyacrylamide gel and then transferred onto a nitrocellulose membrane. Blots were probed with anti-HB9 (H-20, Santa Cruz), anti-turboGFP (cat. #AB 513, Evrogen, Moscow, Russia), anti-phospho-p53(Ser15) (cat. #9284, Cell Signaling, Cambridge, UK), anti-p53 (Ab6, Calbiochem, Darmstadt, Germany), anti-p21 (12D1, Cell Signaling), anti-β-actin (AC-74, Sigma-Aldrich) antibodies at 4°C overnight. After washing with TBS-T, blots were incubated with horseradish peroxidase-conjugated secondary antibodies, donkey-anti-goat IgG-HRP (cat. #2056), goat-anti-mouse IgG-HRP (cat. #2005) and goat-anti-rabbit IgG-HRP (cat. #2004, Santa Cruz), for 2h at RT. Chemiluminescent signals were visualized using Amersham ECL Western Blotting Detection Reagent (GE Healthcare, Frankfurt, Germany) with a LAS3000 transilluminator (GE Healthcare).

PCR and quantitative Reverse Transcriptase-PCR

DNA was extracted from murine peripheral blood using the QIAamp DNA Micro Kit (QIAGEN, Hilden, Germany). PCR analysis to verify genomic vector integration was done using TaqPCR Core Kit (QIAGEN) and the following primer pairs: F-5´-GGACCATTTCCCCTACAGCAA-3´ and R-5´-GTGATGCGGCACTCGATCTC-3´ for HB9-GFP (HB9-vector), F-5´-TGGAGCCTACCTAGACTCAGC-3´ and R-5´-GTGATGCGGCACTCGATCTC-3´ for EF1-GFP (control-vector), F-5´-GACAGCGTGATCTTCACCGA-3´ and R-5´-GTCTTGAAGGCGTGCTGGTA-3´ for GFP (amplification-control).

Total RNA of cell pellets was extracted using the RNeasy Mini or Micro Kit (QIAGEN) and total RNA of murine peripheral blood was extracted using RNeasy Protect Animal Blood Kit (QIAGEN). cDNA synthesis was performed using QuantiTect Reverse Transcription Kit (QIAGEN). Expression analysis was done using TaqMan

Master Mix (Applied Biosystems) and the following primer-probe sets: F-5´-CACCCGCATCGAGAAGTACG-3´, R-5´-CCACCTTGAAGTCGCCGATC-3´ and probe 5´-FAM-CACGTGAGCTTCAGCTACCGCTACGAG-BHQ1-3´ for GFP, multiplexed with F-5´-TCTTTGCAGCTCCTTCGTTGC-3´, R-5´-CACGATGGAGGGGAATACAG-3´ and probe 5´-HEX-CACCCGCAACAAGTTGCGCATGGATG-BHQ1-3´ for murine β-Actin. SybrGreen PCR Master Mix (Applied Biosystems) was used together with the following primer pairs: F-5´-CATGATCCTGCCCAAGATG-3´ and R-5´-GTACCACCTCAAAACGCTTG-3´ for murine HB9; β-Actin primer were the same, as used for probe-based detection. Expression was analyzed using the ddCT method.

Transduction of CD34⁺ cord blood cells

CD34⁺ cells were lentivirally transduced (MOI 50), together with polybrene (5µg/ml) on RetroNectin (Takara, Frankfurt, Germany) coated plates, and spinoculated at 1000g for 2h at 32°C. CD34⁺ cells were sorted by flow cytometry for GFP-expression 72h after transduction and subjected to RNA-Seq analysis.

RNA-Seq analysis

TruSeq RNA Sample Preparation v2 Kit (low-throughput protocol; Illumina, San Diego, CA, USA) was used to prepare the barcoded libraries from 100ng total RNA. Libraries were validated and quantified using DNA 1000 and high-sensitivity chips on Bioanalyzer (Agilent, Böblingen, Germany); 7.5pM denatured libraries were used as input into cBot (Illumina), followed by deep sequencing using HiSeq 2500 (Illumina) for 101 cycles, with an additional 7 cycles for index reading.

Fastq files were imported into Partek Flow. Quality analysis and quality control were performed on all reads to assess read quality and to determine the amount of

trimming required (both ends: 13 bases 5´ and 1 base 3´). Trimmed reads were aligned against the hg38 genome using the STAR v2.4.1d aligner. Unaligned reads were further processed using Bowtie 2 v2.2.5 aligner, and aligned reads were combined before quantifying the expression to the ENSEMBL (release 82 v2) database by the Partek Expectation-Maximization algorithm. Finally, statistical analysis was performed to determine differential expression at both gene and transcript levels. Partek flow defaults were used in all analyses. Genes with a total normalized read count of <12 were excluded from analysis. Genes were defined as HB9-dependent *de novo* expressed by a total normalized read count of ≤1 in GFP- and ≥5 in HB9-GFP-transduced cells. Gene set enrichment analysis (GSEA) was performed using GSEA software using the pre-ranked tool (Broad Institute, Cambridge, MA, USA). All genes which contained an average of more than 1 read across all samples were used and ranked according to the T statistic. Gene sets were comprised of gene ontology terms for biological processes. p values were used in all statistical analyses since sample size was not powered for multiple hypothesis testing.

Antibody panels used for flow cytometric analyses:

Antibodies used with FACS Calibur

Antigen	Dye	Clone	Manufacturer
CD45.2	PerCP-Cy5.5	104	BD Biosciences
CD3e	PE	145-2C11	BD Biosciences
CD3e	APC	145-2C11	BD Biosciences
CD4	APC	RM4-5	BD Biosciences
CD8b.2	PE	53-5.8	BD Biosciences
TCRβ	PE	H57-597	BD Biosciences
CD19	PE	1D3	BD Biosciences
IgM	APC	II/41	BD Biosciences
IgD	APC	11-26c.2a	BD Biosciences
Gr-1	APC	RB6-8C5	BD Biosciences
Nk-1.1	PE	PK136	BD Biosciences
CD45.1	PE	A20	BD Biosciences
CD11b	PE	M1/70	BD Biosciences

Stem-/progenitor cell panel used with CyAn ADP Analyzer

Antigen	Dye	Clone	Manufacturer
Sca-1 (Ly-6A/E)	PE	D7	BD Biosciences
CD135 (Flk-2)	PE-CF594	A2F10.1	BD Biosciences
Lin-	Biotin	#130-092-613	Miltenyi Biotec
CD45.1	Biotin	A20	BD Biosciences
Biotin	PerCP-Cy5.5	#551419	BD Biosciences
CD127 (IL7Rα)	PE-Cy7	SB/199	BD Biosciences
CD34	Alexa Fluor 647	RAM-34	BD Biosciences
CD16/CD32 (FcγR)	eFluor 450	93	eBioscience (Frankfurt a. M., Germany)
CD117 (c-Kit)	APC-H7	2B8	BD Biosciences

B-cell panel used with CyAn ADP Analyzer

Antigen	Dye	Clone	Manufacturer
CD43	PE	S7	BD Biosciences
Early B lineage (CD93)	PE-CF594	AA4.1	BD Biosciences
CD45.2	PerCP-Cy5.5	104	BD Biosciences
IgM	PE-Cy7	R6-60.2	BD Biosciences
IgD	APC	11-26c.2a	BD Biosciences
CD45R/B220	eFluor 450	RA3-6B2	eBioscience
CD19	APC-H7	1D3	BD Biosciences

## T-cell panel used with CyAn ADP Analyzer

Antigen	Dye	Clone	Manufacturer
CD8	PE	53-5.8	BD Biosciences
CD4	PE-CF594	RM4-5	BD Biosciences
CD45.2	PerCP-Cy5.5	104	BD Biosciences
Ter119	PE-Cy7	TER-119	BD Biosciences
CD3e	APC	145-2C11	BD Biosciences
TCRβ	eFluor 450	H57-597	eBioscience

Myeloid cell panel used with CyAn ADP Analyzer

| Antigen	Dye	Clone	Manufacturer
F4/80 Like Receptor	PE	6F12	BD Biosciences
CD11b	PE-CF594	M1/70	BD Biosciences
CD45.2	PerCP-Cy5.5	104	BD Biosciences
Nk-1.1	PE-Cy7	PK136	BD Biosciences
Ly-6G	APC	1A8	BD Biosciences
Ly-6C	eFluor450	HK1.4	eBioscience
CD11c	APC-Cy7	HL3	BD Biosciences

Supplementary Figures

Figure S1
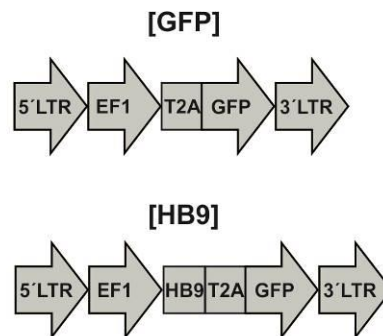
Figure S1: Lentiviral expression cassettes.

Shown are the expression cassettes of the lentiviral expression vectors used for transduction, containing HB9-GFP [HB9] or GFP [GFP] coding sequence, driven by EF1 promoter.
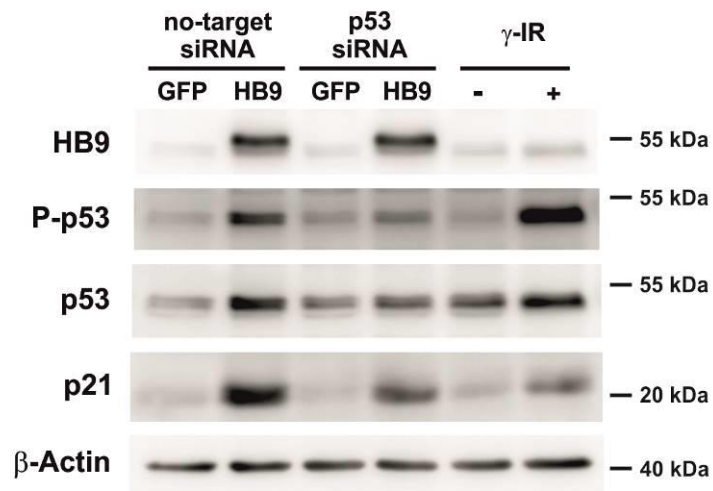
Figure S2
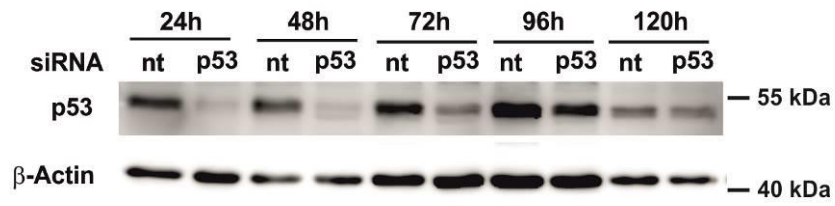
Figure S2: Kinetics of siRNA-mediated p53 knockdown in HT1080 cells.

HT1080 cells were transfected with p53- or non-targeting (nt) siRNA and analyzed for p53 expression by immunoblotting 24–120h post transfection. β-Actin served as loading control.
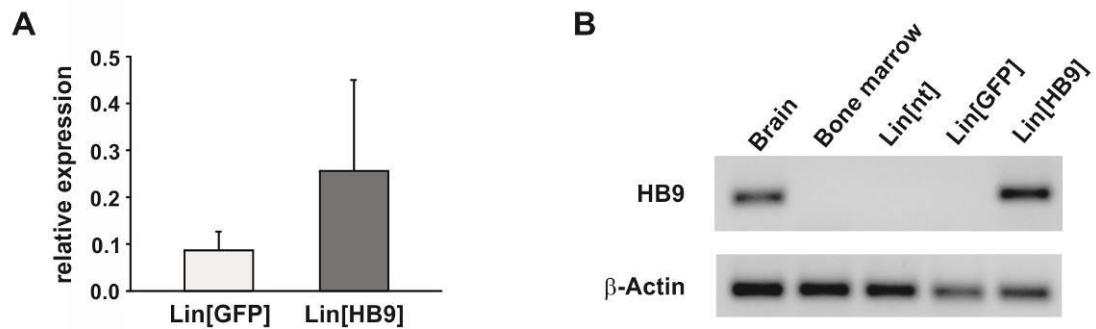
Figure S3

Figure S3: Western blot analysis of p53/p21-signaling in HB9-transduced HT1080 cells after p53 knockdown.

Immunoblot analysis of p53, phosphorylated p53 at Ser15 (P-p53) and p21 in HB9-GFP- or GFP-transduced HT1080 cells, 72h after transfection with non-targeting or p53-targeting siRNA. γ-irradiated (10Gy) cells serve as positive control for p53 pathway activation. β-Actin served as loading control. Shown is one representative experiment out of three.

**Figure S4**: Control of transduction in murine Lin⁻ cells.

(A) qRT-PCR analysis of GFP expression in HB9-GFP- or GFP-transduced Lin⁻ cells 72h after transduction. Expression was normalized to β-Actin (n=3).

(B) Reverse Transcriptase-PCR of HB9 and β-Actin expression in murine bone marrow, non-(nt), HB9- or GFP-transduced Lin⁻ cells. Murine brain tissue served as positive control.
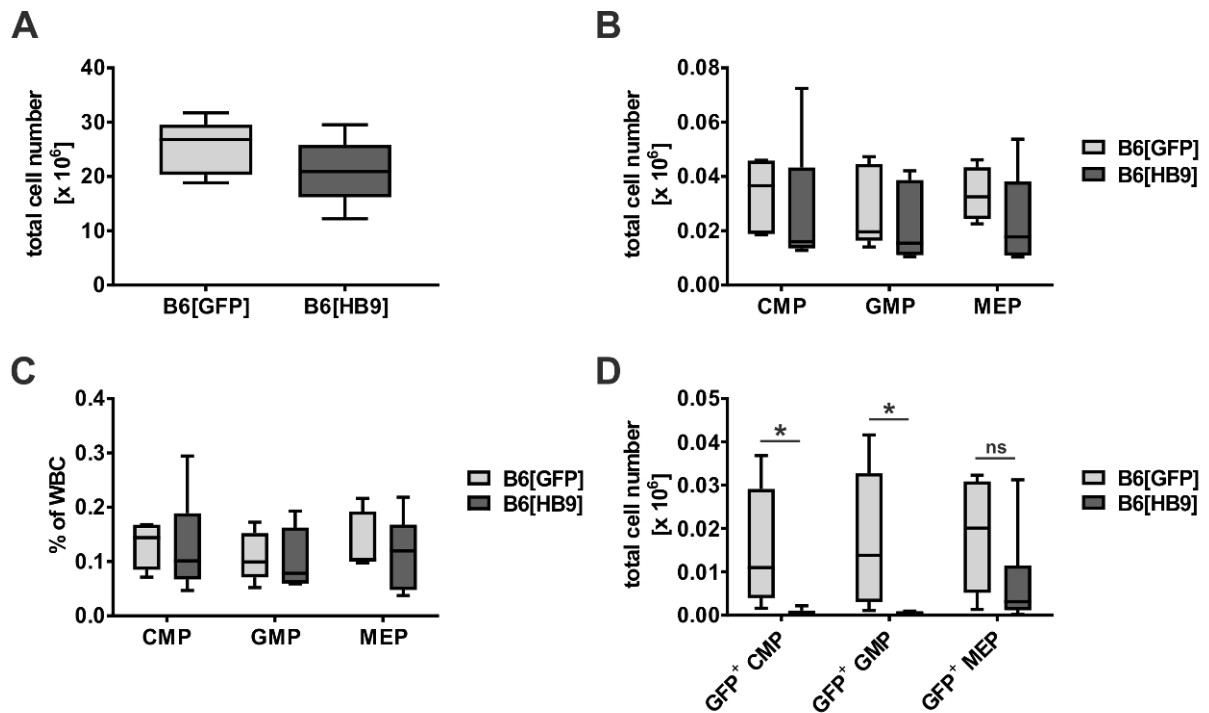
Figure S5
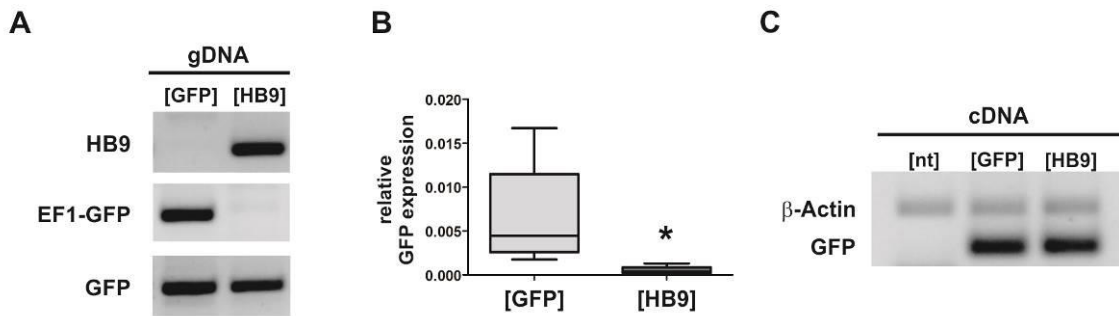
Figure S5: Confirmation of vector integration and expression in peripheral blood cells of transplanted mice.

(A) PCR was conducted to confirm genomic integration of HB9 or GFP vector expression cassettes. **(B)** qRT-PCR analysis of GFP expression in peripheral blood cells of Lin[GFP]- ([GFP]) or Lin[HB9]-transplanted ([HB9]) mice (n=6) and subsequent gel electrophoretic analysis **(C)**. Shown is one representative experiment. PCR regarding vector integration and expression was conducted for each transplanted animal.

Figure S6

**Figure S6**: Total bone marrow cell numbers of B6[GFP] and B6[HB9] mice in myeloid progenitor populations.

(A) Total number of white blood cells in bone marrow of B6[GFP] and B6[HB9] mice (n=5). **(B)** Total cell numbers and **(C)** frequencies of CMP, GMP and MEP in B6[GFP] and B6[HB9] mice (n=5). **(D)** Total cell number of HB9-GFP+/GFP+ CMP, GMP and MEP in B6[GFP] and B6[HB9] mice (n=5). ns = not significant.

Figure S7

A CD45.2 staining

B B-cell staining

C T-cell staining
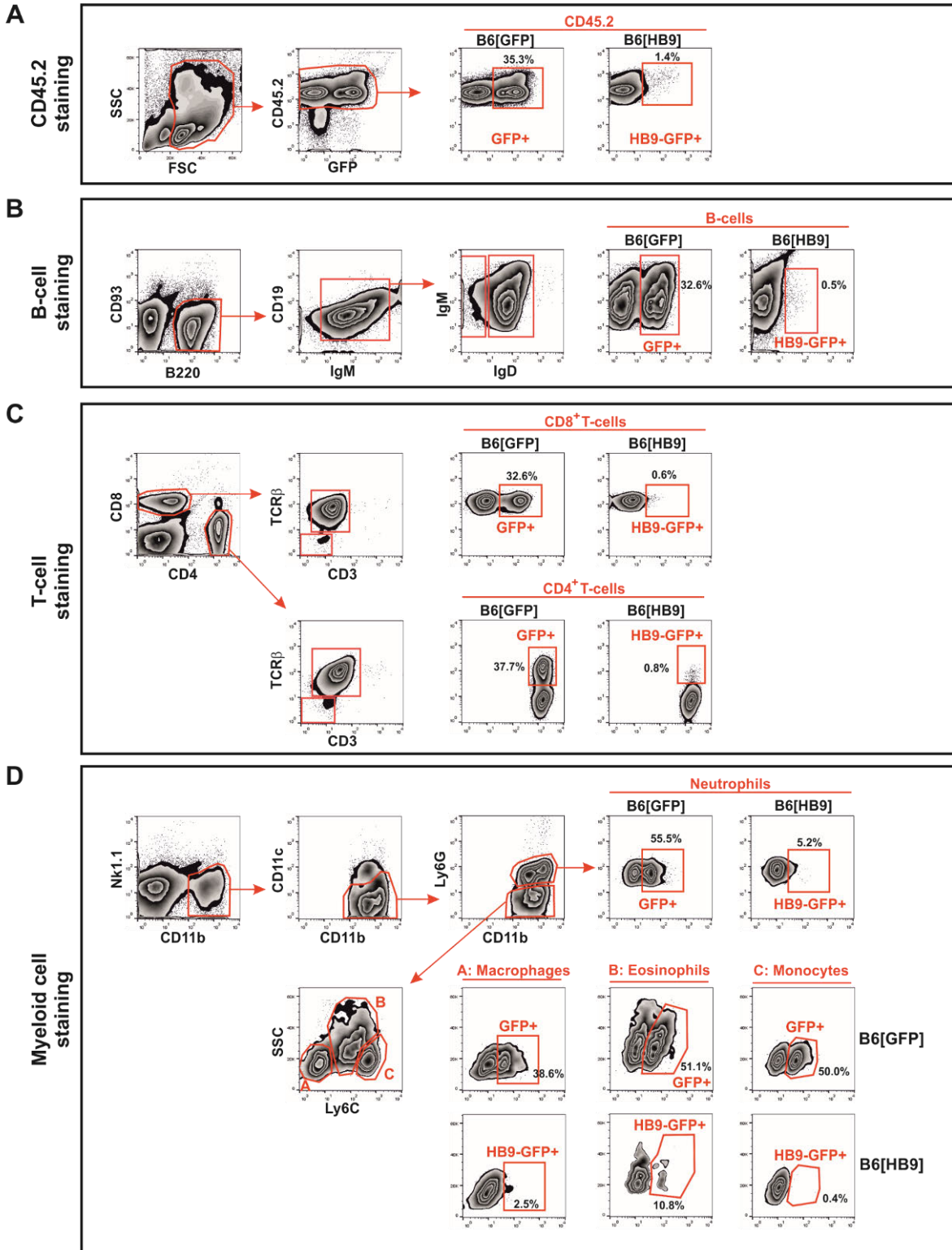
D Myeloid cell staining
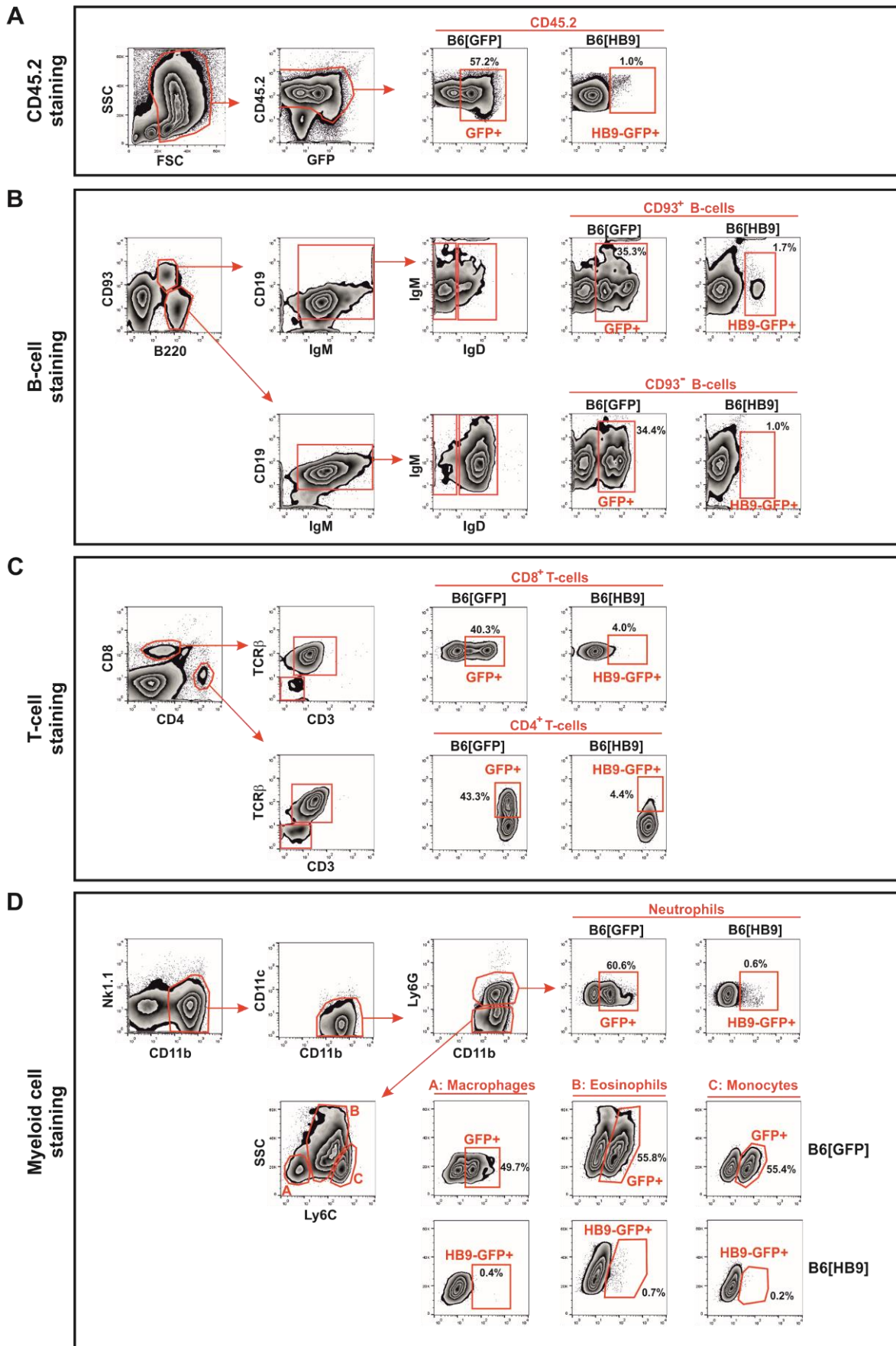
Figure S7: Flow cytometric gating strategy for murine bone marrow cell analysis of transplanted mice.

Murine bone marrow leukocytes were gated for CD45.2 (**A**), followed by gating regarding lineage specific markers for B-cells (**B**), T-cells (**C**) and myeloid cells (**D**), together with GFP. For B-cell analysis, B220$^+$ cells were subdivided into immature (CD93$^+$) and more mature (CD93$^-$) B-cells, which were further analyzed for CD19, IgM and IgD expression. T-cells were subdivided into CD8$^+$ and CD4$^+$ T-cells and further analyzed regarding TCRβ and CD3 expression. For myeloid cell analysis, CD11b$^+$ Nk1.1$^-$ CD11c$^-$ cells were analyzed for Ly-6G expression to identify neutrophils. Ly-6G$^-$ cells were further analyzed regarding granularity and Ly-6C expression to distinguish between macrophages (Ly-6C$^{low-neg}$ SSC^{low}), monocytes (Ly-6C$^+$ SSC^{low}) and eosinophils (Ly-6C$^{low-neg}$ SSC^{high}) [2].
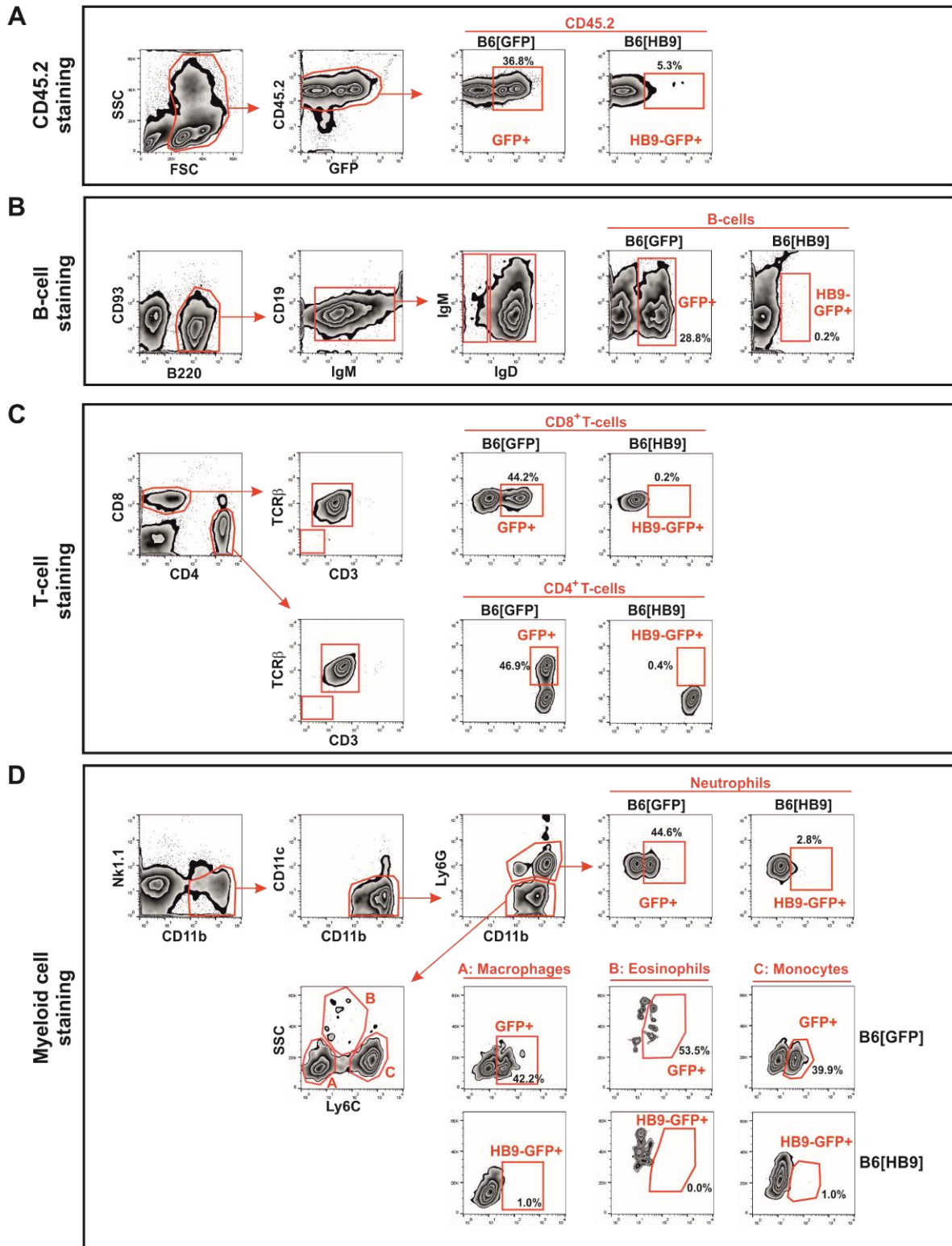
Figure S8

Figure S8: Flow cytometric gating strategy for murine splenocyte analysis of transplanted mice.

Murine splenic leukocytes were gated for CD45.2 (**A**), followed by gating regarding lineage specific markers for B-cells (**B**), T-cells (**C**) and myeloid cells (**D**), together with GFP. For B-cell analysis, B220$^+$ B-cells were further analyzed for CD19, IgM and IgD expression. T-cells were subdivided into CD8$^+$ and CD4$^+$ T-cells and further analyzed regarding TCRβ and CD3 expression. For myeloid cell analysis, CD11b$^+$ Nk1.1$^-$ CD11c$^-$ cells were analyzed for Ly-6G expression to identify neutrophils. Ly-6G$^-$ cells were further analyzed regarding granularity and Ly-6C expression to distinguish between macrophages (Ly-6C$^{low-neg}$ SSC^{low}), monocytes (Ly-6C$^+$ SSC^{low}) and eosinophils (Ly-6C$^{low-neg}$ SSC^{high}) [2].

Figure S9

A — CD45.2 staining
SSC vs FSC; CD45.2 vs GFP; B6[GFP] 36.8% GFP+; B6[HB9] 5.3% HB9-GFP+; CD45.2

B — B-cell staining
CD93 vs B220; CD19 vs IgM; IgM vs IgD; B-cells; B6[GFP] 28.8% GFP+; B6[HB9] 0.2% HB9-GFP+

C — T-cell staining
CD8 vs CD4; TCRβ vs CD3; CD8+ T-cells; B6[GFP] 44.2% GFP+; B6[HB9] 0.2% HB9-GFP+; TCRβ vs CD3; CD4+ T-cells; B6[GFP] 46.9% GFP+; B6[HB9] 0.4% HB9-GFP+

D — Myeloid cell staining
Nk1.1 vs CD11b; CD11c vs CD11b; Ly6G vs CD11b; Neutrophils; B6[GFP] 44.6% GFP+; B6[HB9] 2.8% HB9-GFP+; SSC vs Ly6C (A, B, C); A: Macrophages B6[GFP] 42.2% GFP+, B6[HB9] 1.0% HB9-GFP+; B: Eosinophils B6[GFP] 53.5% GFP+, B6[HB9] 0.0% HB9-GFP+; C: Monocytes B6[GFP] 39.9% GFP+, B6[HB9] 1.0% HB9-GFP+
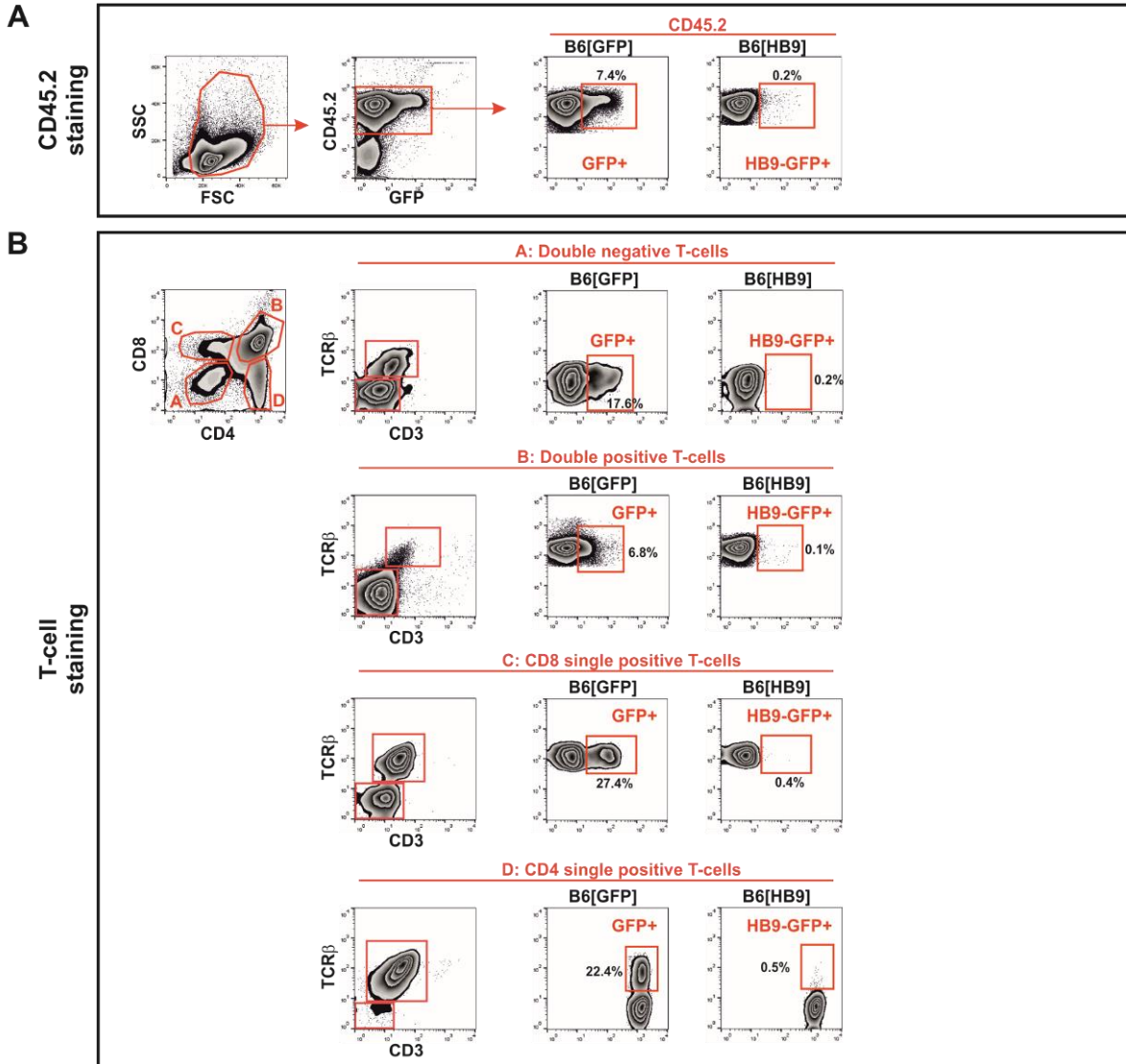
19

Figure S9: Flow cytometric gating strategy for murine peripheral blood analysis of transplanted mice.

Murine peripheral blood leukocytes were gated for CD45.2 (**A**), followed by gating regarding lineage specific markers for B-cells (**B**), T-cells (**C**) and myeloid cells (**D**), together with GFP. For B-cell analysis, B220$^+$ B-cells were further analyzed for CD19, IgM and IgD expression. T-cells were subdivided into CD8$^+$ and CD4$^+$ T-cells and further analyzed regarding TCRβ and CD3 expression. For myeloid cell analysis, CD11b$^+$ Nk1.1$^-$ CD11c$^-$ cells were analyzed for Ly-6G expression to identify neutrophils. Ly-6G$^-$ cells were further analyzed regarding granularity and Ly-6C expression to distinguish between macrophages (Ly-6C$^{low-neg}$ SSC^{low}), monocytes (Ly-6C$^+$ SSC^{low}) and eosinophils (Ly-6C$^{low-neg}$ SSC^{high}) [2].

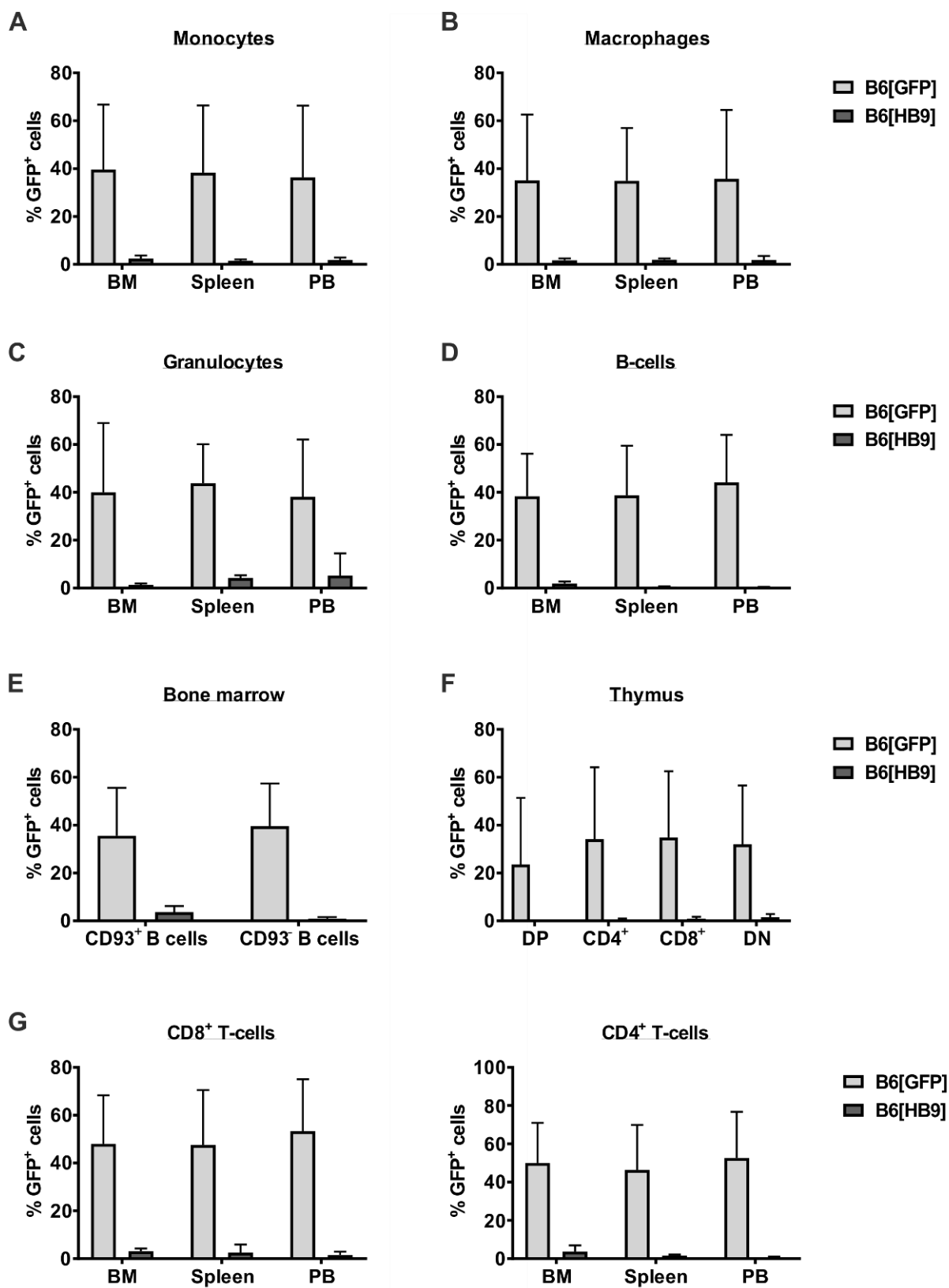**Figure S10**

Figure S10: Flow cytometric gating strategy for murine thymocyte analysis of transplanted mice.

Murine thymocytes were gated for CD45.2 (**A**), followed by gating regarding CD8 and CD4 expression to distinguish between double-negative, double-positive and CD8/CD4 single positive T-cells (**B**). Each subpopulation was further analyzed regarding TCRβ, CD3 and GFP.
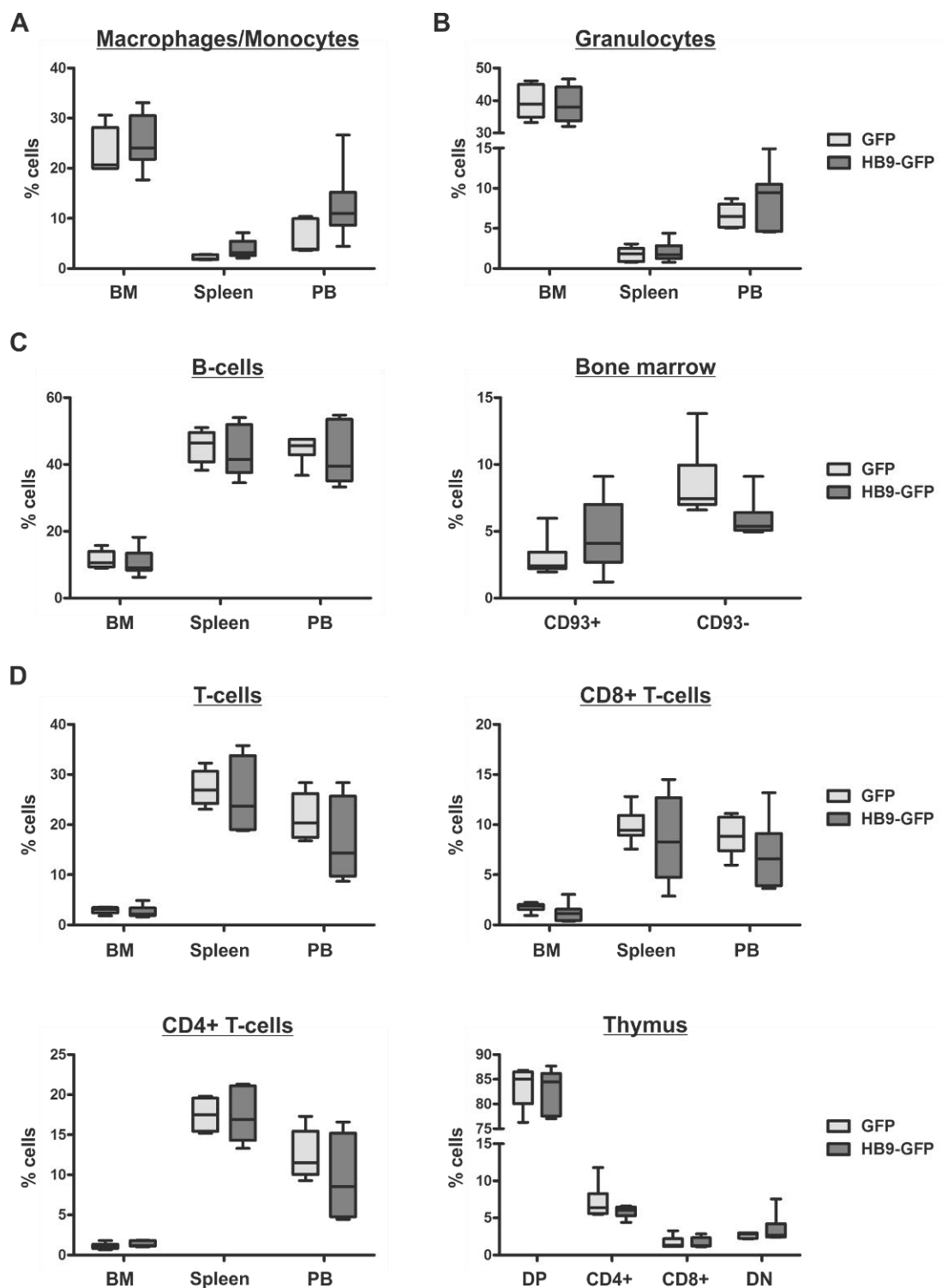
Figure S11

Figure S11: GFP$^+$ cell frequencies of lymphoid and myeloid cell types in bone marrow, spleen, thymus and peripheral blood of B6[GFP] and B6[HB9].

Flow cytometric analysis was used to determine the GFP$^+$ cell frequency of total monocytes (CD11b$^+$Nk1.1$^-$CD11c$^-$Ly-6G$^-$Ly-6C$^+$SSC^{low}) (**A**), macrophages (CD11b$^+$Nk1.1$^-$CD11c$^-$Ly-6G$^-$Ly-6C$^{low-neg}$SSC^{low}) (**B**), granulocytes (**C**), B-cells (B220$^+$) (**D**) and CD8$^+$/CD4$^+$ T-cells (**G**) in bone marrow (BM), spleen and peripheral blood (PB) of B6[GFP] and B6[HB9]. Granulocytes are cumulated of neutrophils (CD11b$^+$Nk1.1$^-$CD11c$^-$Ly-6G$^+$) and eosinophils (CD11b$^+$Nk1.1$^-$CD11c$^-$Ly-6G$^-$Ly-6C$^{low-neg}$SSC^{high}). To investigate GFP$^+$ cell frequency of developing B-cells, B220$^+$ BM cells were subdivided into immature (CD93$^+$) and more mature (CD93$^-$) B-cells (**E**). With regard to T-cell maturation, GFP$^+$ cell frequencies were assessed in thymocytes, starting from CD4/CD8 double-negative (DN), to CD4/CD8 double-positive (DP) and finally CD4/CD8 single positive T-cells (**F**).
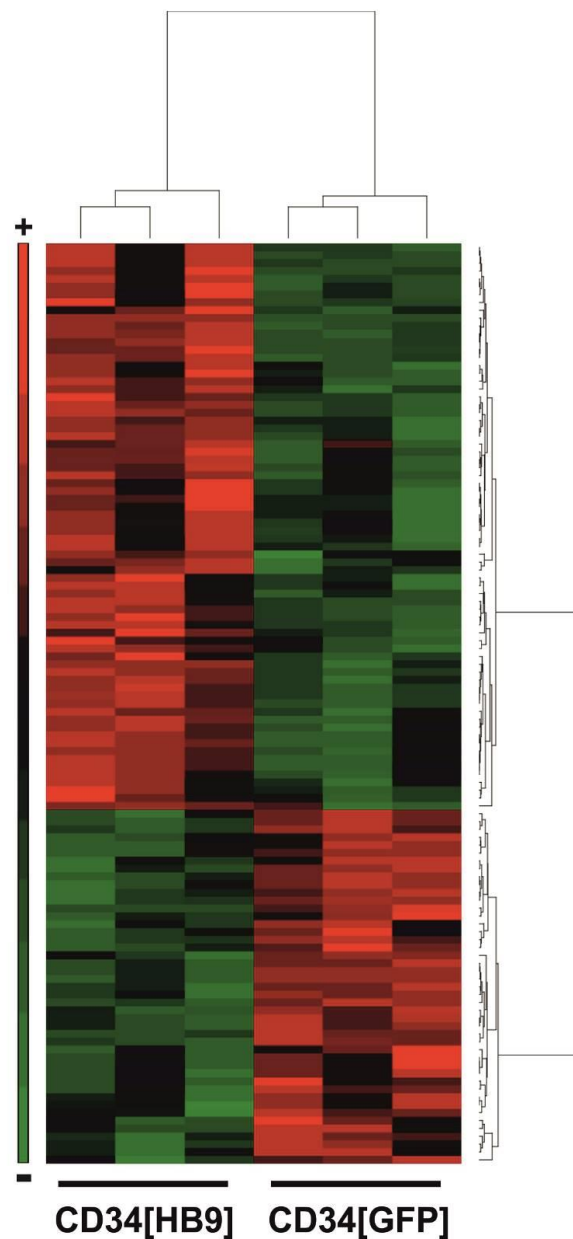
Figure S12

Figure S12: Frequency of lymphoid and myeloid cell types in bone marrow, spleen, thymus and peripheral blood of B6[GFP] and B6[HB9].

Flow cytometric analysis was used to determine the frequency of total macrophages/monocytes (CD11b$^+$Nk1.1$^-$CD11c$^-$Ly-6G$^-$Ly-6C$^{-/+}$SSC^{low}) **(A)**, granulocytes **(B)**, B-cells (B220$^+$) (**C**), total T-cells (CD3$^+$TCRβ$^+$), as well as CD8$^+$/CD4$^+$ T-cells (**D**) in CD45.2$^+$ bone marrow cells (BM), splenocytes and peripheral blood cells (PB) of B6[GFP] and B6[HB9]. Total granulocyte frequency was cumulated of neutrophils (CD11b$^+$Nk1.1$^-$CD11c$^-$Ly-6G$^+$) and eosinophils (CD11b$^+$Nk1.1$^-$CD11c$^-$Ly-6G$^-$Ly-6C$^{low-neg}$SSC^{high}). For bone marrow analysis, B-cells were further subdivided into immature (B220$^+$CD93$^+$) and more mature (B220$^+$CD93$^-$) B-cells (**C**). Thymus was analyzed with respect to different T-cell maturation stages, starting from CD4/CD8 double-negative (DN), to CD4/CD8 double-positive (DP) and resulting in CD4/CD8 single positive T-cells (**D**).

Figure S13

Figure S13: Hierarchical clustering analysis of differentially expressed genes in CD34[HB9] compared to CD34[GFP].

Hierarchical clustering analysis of differentially expressed genes (p≤0.05) shows distinct clustering of HB9- as well as GFP-transduced CD34+ HSPCs. Upregulated genes are depicted in red and downregulated genes are depicted in green.

Figure S14
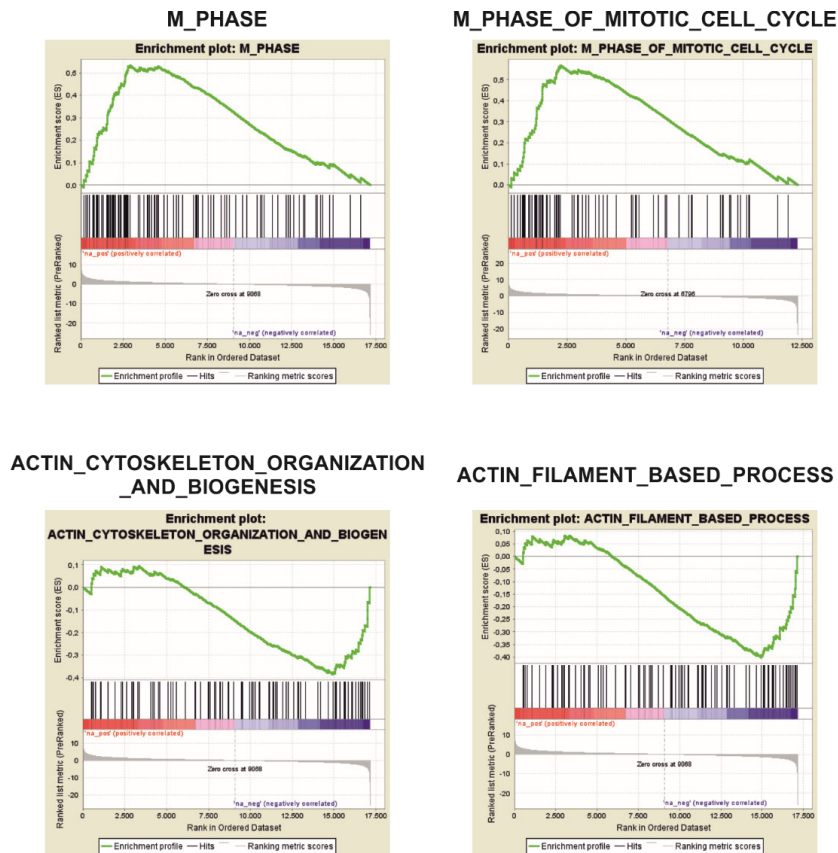
Figure S14: Gene set enrichment analysis of up- and down-regulated genes in CD34[HB9] based on their biological process annotations.

Gene set enrichment analysis plots show upregulation of M-phase process-related genes and downregulation of actin-based process-related genes in CD34[HB9] compared to CD34[GFP].
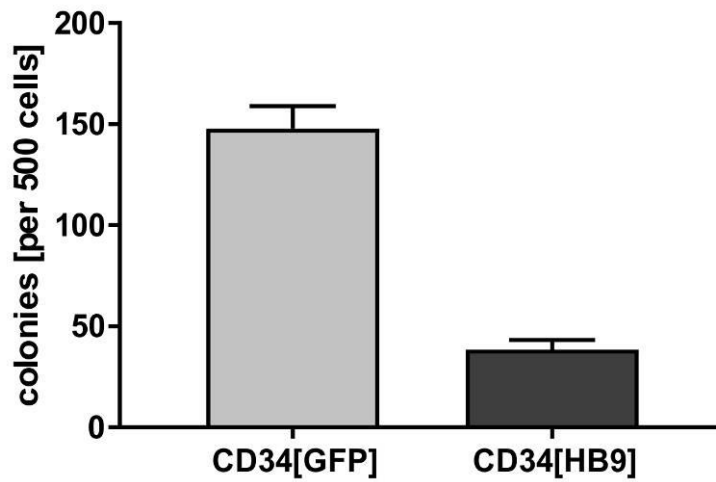
Figure S15: Evaluation of clonogenicity in CD34[HB9] compared to CD34[GFP].

500 cells were seeded per condition. Shown is one biological experiment including

six technical replicates. Experiment were conducted as written elsewhere [3].

Figure S16
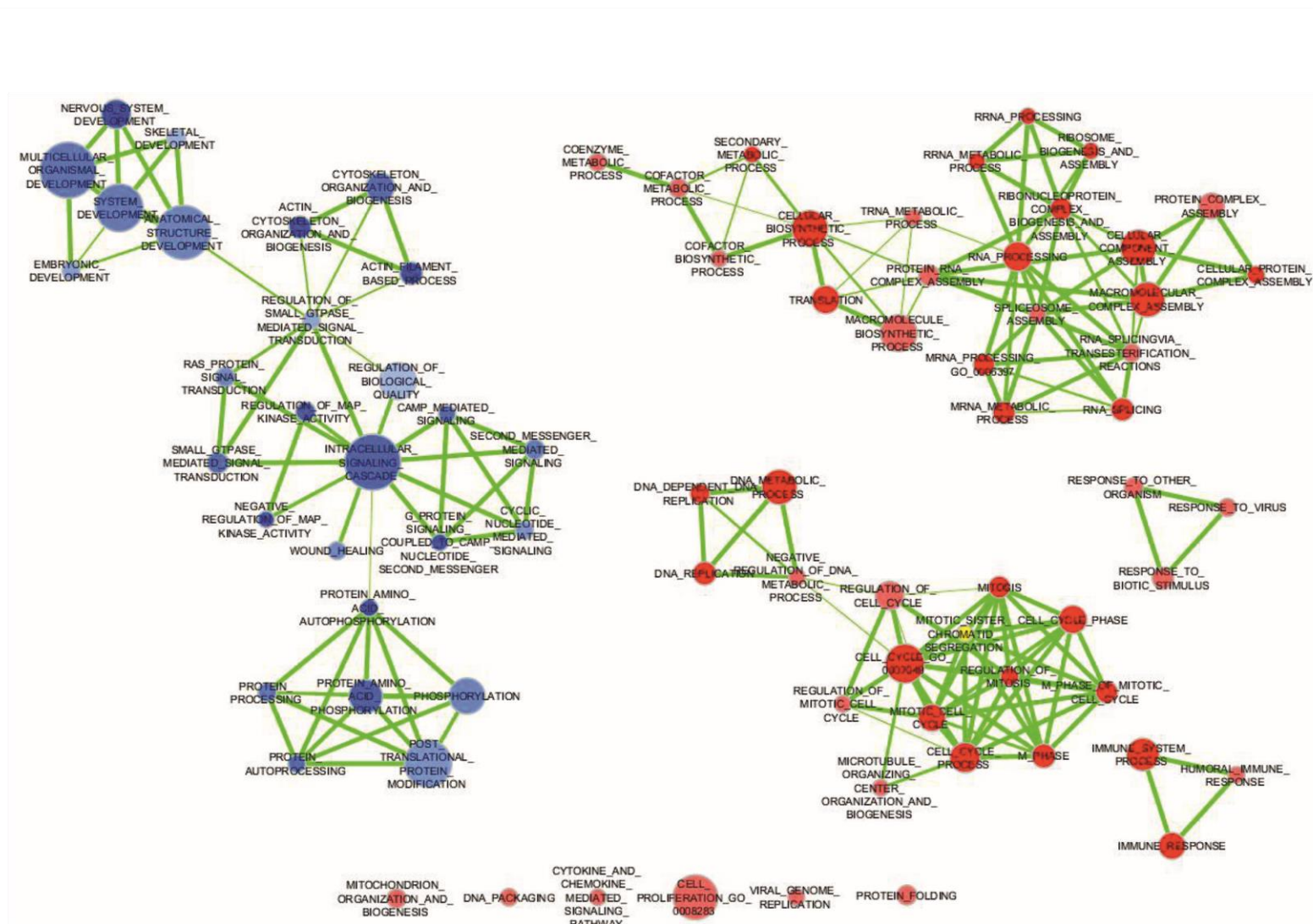
Figure S16: Network of differentially regulated biological processes in CD34[HB9] compared to CD34[GFP].

Significantly (p≤0.05) differentially regulated biological process GO-terms identified between CD34[HB9] and CD34[GFP] are visualized in a network using Cytoscape software. HB9-dependent positively enriched biological processes are depicted in red and HB9-dependent negatively enriched biological processes are depicted in blue. Circle size is relative to the number of genes affected and thickness of lines connecting two circles is indicative of the number of genes shared between these two GO-terms.

Table S1: HB9-dependent differentially regulated genes in CD34[HB9] compared to CD34[GFP].

Shown are 117 genes, which are significantly (p≤0.05) differentially expressed with a fold change (FC) ≥ 1.8 in CD34[HB9] compared to CD34[GFP]. HB9-dependent upregulated genes are depicted in red and HB9-dependent downregulated genes are depicted in green.

Table S1

chr.	gene	p-value	FC		chr.	gene	p-value	FC
7	MNX1	2.37E-06	1998.36		11	MPZL2	4.91E-02	1.94
16	HBZ	1.18E-04	259.25		10	MYOF	3.11E-02	1.93
16	MT1G	4.86E-03	67.76		1	SLC2A5	1.13E-02	1.92
17	SLC4A1	2.19E-04	27.29		22	GGT5	4.82E-02	1.92
20	BPI	4.21E-02	27.14		7	FAM188B	9.39E-03	1.91
16	MT1X	4.50E-03	21.04		21	JAM2	4.65E-02	1.90
7	AQP1	4.28E-03	18.10		15	CTSH	3.40E-02	1.90
8	FAM83A	1.38E-02	15.47		1	PADI4	4.00E-02	1.89
16	CCL22	4.10E-02	12.99		10	CDH23	4.39E-02	1.87
16	HBA2	1.24E-02	12.37		16	NOL3	3.16E-02	1.85
16	HBA1	1.38E-03	12.09		4	JCHAIN	1.07E-02	1.85
16	MT2A	1.66E-02	9.79		19	ICAM1	2.37E-02	1.84
19	PALM3	1.44E-03	8.63		11	HBD	4.05E-03	1.82
19	C3	3.72E-03	8.15		14	PTGER2	7.38E-03	-1.80
5	ADAM19	5.54E-03	6.74		8	CYP7B1	4.87E-02	-1.81
14	SLC7A8	7.73E-03	5.77		15	RAD51-AS1	1.94E-02	-1.81
20	MMP9	7.31E-03	5.46		9	PIP5K1B	6.04E-03	-1.81
2	IGFBP5	2.25E-02	5.44		6	SYTL3	1.48E-03	-1.84
X	ALAS2	6.95E-04	5.17		6	MYLK4	2.59E-03	-1.86
14	ASB2	1.59E-03	4.78		1	LAX1	4.37E-03	-1.86
19	SEMA6B	7.29E-03	4.78		3	LXN	6.66E-04	-1.87
11	HBE1	1.92E-02	4.55		10	FAM171A1	2.73E-02	-1.87
6	CD24	3.66E-02	4.36		12	PDE3A	4.73E-02	-1.87
17	HIC1	9.66E-03	4.26		2	TRIB2	2.19E-03	-1.87
8	NEFM	3.12E-03	4.00		3	SLC9A9	3.97E-02	-1.89
11	LRRC32	1.66E-02	3.50		8	DLC1	5.42E-03	-1.90
8	DUSP4	3.44E-04	3.38		1	SPTA1	4.01E-02	-1.91
11	TSPAN18	1.18E-02	3.19		18	RAB27B	3.26E-03	-1.93
2	LONRF2	1.76E-03	3.12		4	LEF1	3.15E-02	-1.98
20	THBD	3.77E-02	2.96		11	VWA5A	3.83E-02	-2.00
2	NMUR1	1.23E-02	2.79		2	FAM178B	2.93E-02	-2.01
4	NAT8L	4.72E-03	2.76		1	FCER1A	3.08E-02	-2.02
19	LILRB4	2.20E-02	2.68		19	PLVAP	8.93E-03	-2.05
3	PLXNA1	2.46E-02	2.65		2	LTBP1	3.62E-03	-2.05
21	PDE9A	2.07E-03	2.65		8	FZD3	1.12E-02	-2.06
10	IL2RA	5.17E-03	2.56		1	TGFBR3	1.96E-02	-2.12
1	SLC30A1	1.58E-02	2.48		8	IL7	2.35E-03	-2.12
6	LTB	7.09E-03	2.47		4	HPGD	3.28E-02	-2.13
16	ADGRG5	1.69E-02	2.47		6	CNKSR3	4.89E-03	-2.13
2	GPR35	1.65E-02	2.43		2	DPP4	4.73E-02	-2.14
3	EPHB3	1.01E-03	2.43		8	CA1	4.07E-02	-2.23
22	A4GALT	1.44E-02	2.43		18	SLC14A1	1.73E-02	-2.24
5	CD180	5.66E-03	2.41		9	TEK	4.82E-02	-2.25
17	CCR7	7.60E-03	2.39		7	CD36	3.16E-03	-2.36
16	ADGRG3	6.49E-03	2.38		7	DPY19L2P1	3.62E-02	-2.40
17	ABI3	3.55E-02	2.38		17	CDRT4	3.62E-02	-2.45
X	VSIG4	6.53E-03	2.36		16	CALB2	4.27E-02	-2.62
6	IRF4	9.49E-03	2.23		1	PCSK9	8.62E-03	-2.72
16	HBQ1	5.32E-03	2.23		12	SLC2A14	1.40E-02	-2.80
2	MYO1B	2.49E-02	2.20		7	ITGB8	1.05E-02	-2.84
11	HBG2	1.88E-02	2.15		15	FBN1	6.33E-04	-2.88
14	SERPINA1	3.85E-02	2.15		6	PLEKHG1	8.76E-03	-3.13
1	DHRS3	2.39E-02	2.14		6	CRISP3	4.13E-02	-3.28
10	TSPAN15	1.89E-02	2.14		13	TNFRSF19	1.92E-02	-3.45
7	UPP1	2.79E-02	2.11		19	CLC	7.07E-04	-3.47
17	LGALS3BP	3.58E-02	2.07		9	FREM1	4.57E-02	-3.55
12	TESC	8.48E-03	2.05		17	FOXJ1	1.95E-03	-3.99
12	ITGB7	1.68E-02	2.05		15	RYR3	1.63E-02	-8.21
11	HBBP1	6.68E-04	2.02					

Table S2: Gene set enrichment analysis of up- and down-regulated genes in CD34[HB9] based on their biological process annotations.

Shown here are the most significant (p≤0.01) biological processes enriched in CD34[HB9] compared to CD34[GFP], with respect to the normalized enrichment score (NES).

Table S2

GO-term	NES	p-value
M_PHASE	20.90	<0.0001
M_PHASE_OF_MITOTIC_CELL_CYCLE	20.83	<0.0001
MITOSIS	20.50	<0.0001
RIBONUCLEOPROTEIN_COMPLEX_BIOGENESIS_AND_ASSEMBLY	19.77	<0.0001
RNA_SPLICING	19.67	<0.0001
RIBOSOME_BIOGENESIS_AND_ASSEMBLY	19.66	<0.0001
DNA_REPLICATION	19.10	<0.0001
RRNA_PROCESSING	18.92	0.0026
RRNA_METABOLIC_PROCESS	18.69	0.0028
CELLULAR_PROTEIN_COMPLEX_ASSEMBLY	18.19	<0.0001
RNA_PROCESSING	18.11	<0.0001
SECONDARY_METABOLIC_PROCESS	17.96	0.0018
REGULATION_OF_MITOSIS	17.76	0.0035
CYTOKINE_AND_CHEMOKINE_MEDIATED_SIGNALING_PATHWAY	17.24	0.0088
CELL_CYCLE_GO_0007049	17.04	<0.0001
DNA_METABOLIC_PROCESS	16.61	<0.0001
MRNA_METABOLIC_PROCESS	16.48	0.0043
CELL_CYCLE_PHASE	16.42	<0.0001
TRANSLATION	16.34	0.0008
MITOTIC_CELL_CYCLE	16.23	0.0016
RESPONSE_TO_OTHER_ORGANISM	16.19	0.0059
COFACTOR_METABOLIC_PROCESS	16.18	0.0095
PROTEIN_RNA_COMPLEX_ASSEMBLY	15.85	0.0100
IMMUNE_RESPONSE	15.26	0.0024
CELLULAR_COMPONENT_ASSEMBLY	15.06	<0.0001
IMMUNE_SYSTEM_PROCESS	14.98	0.0048
CELLULAR_BIOSYNTHETIC_PROCESS	14.95	0.0024
MACROMOLECULAR_COMPLEX_ASSEMBLY	14.78	0.0016
INTRACELLULAR_SIGNALING_CASCADE	-13.37	0.0016
MULTICELLULAR_ORGANISMAL_DEVELOPMENT	-13.38	0.0031
PHOSPHORYLATION	-14.53	0.0042
NERVOUS_SYSTEM_DEVELOPMENT	-15.18	<0.0001
PROTEIN_AMINO_ACID_PHOSPHORYLATION	-15.47	0.0014
REGULATION_OF_MAP_KINASE_ACTIVITY	-15.93	0.0093
PROTEIN_AMINO_ACID_AUTOPHOSPHORYLATION	-17.08	0.0058
RAS_PROTEIN_SIGNAL_TRANSDUCTION	-17.27	0.0047
WOUND_HEALING	-17.65	0.0046
PROTEIN_PROCESSING	-17.72	0.0033
G_PROTEIN_SIGNALING_COUPLED_TO_CAMP_NUCLEOTIDE_SECOND_MESSENGER	-17.89	0.0057
SMALL_GTPASE_MEDIATED_SIGNAL_TRANSDUCTION	-18.05	0.0023
NEGATIVE_REGULATION_OF_MAP_KINASE_ACTIVITY	-18.37	0.0056
PROTEIN_AUTOPROCESSING	-18.43	0.0023
ACTIN_CYTOSKELETON_ORGANIZATION_AND_BIOGENESIS	-18.44	<0.0001
ACTIN_FILAMENT_BASED_PROCESS	-18.76	<0.0001

References

1.	Dull T, Zufferey R, Kelly M, et al. A third-generation lentivirus vector with a conditional packaging system. J Virol. 1998;72(11):8463-8471.
2.	Rose S, Misharin A, Perlman H. A novel Ly6C/Ly6G-based strategy to analyze the mouse splenic myeloid compartment. Cytometry Part A : the journal of the International Society for Analytical Cytology. 2012;81(4):343-350.
3.	Bhatia S, Reister S, Mahotka C, Meisel R, Borkhardt A, Grinstein E. Control of AC133/CD133 and impact on human hematopoietic progenitor cells through nucleolin. Leukemia. 2015;29(11):2208-2220.